Nanoscale

ROYAL SOCIETY OF CHEMISTRY

COMMUNICATION

View Article Online
View Journal | View Issue

Cite this: *Nanoscale*, 2023, **15**, 8972

Received 14th March 2023,
Accepted 19th April 2023

DOI: 10.1039/d3nr01175e

rsc.li/nanoscale

^{19}F NMR ON/OFF nanoparticles: a universal approach for the specific detection of DNA-binding cancer biomarkers†

Devanathan Perumal, Jithu Krishna, Kaloor S. Harikrishnan, Gowtham Raj, Jemshiya Kalathil, Minu Saji, Kavyasree M. and Reji Varghese *

A supramolecular approach for the design of assembly–disassembly-driven ^{19}F ON/OFF nanoparticles, triggered by specific molecular recognition, for the detection of DNA binding cancer biomarkers is reported. The key to our design strategy is the characteristic ^{19}F NMR signal of the probe, which completely vanishes in the aggregated state due to the shortening of T_2 relaxation. However, molecular recognition of DNA by the cancer biomarkers through specific molecular recognition results in the disassembly of the nanoparticles, which causes the restoration of the characteristic ^{19}F signal of the probe. The universal nature of the approach is demonstrated through the selective detection of various cancer biomarkers including miRNA, ATP, thrombin, and telomerase.

Early-stage and precise diagnosis of cancer is extremely important for its successful treatment.[1] Biomarker-targeted *in vitro* detection of cancer is undoubtedly one of the most promising non-invasive approaches for cancer diagnosis.[2] Recent years have witnessed substantial growth in this field and different detection strategies based on colorimetry,[3] fluorescence,[4] electrochemical,[5] enzyme-linked immunosorbent assay (ELISA),[6] polymerase chain reaction (PCR),[7] and surface enhanced Raman spectroscopy (SERS)[8] have been developed. Although robust and highly efficient, most of them still suffer from a lack of sensitivity and specificity. Hence, there is always a rising demand for the development of *in vitro* biosensors that allow cancer diagnosis with extremely high precision and sensitivity. Among the various non-invasive diagnostic tools available for cancer diagnosis, ^{19}F magnetic resonance imaging (^{19}F MRI) has attracted enormous attention. This is mainly due to the following reasons: (i) high sensitivity (83% relative to ^{1}H), (ii) 100% natural abundance, and (iii) essentially no ^{19}F in animal bodies and hence no background signals.[9–11] Though few strategies have been reported for the design of ^{19}F-based biosensors, this area is still in its infancy.

One of the remarkable features of ^{19}F is the large chemical shift distribution and hence even a small perturbation in the chemical shift produces distinct ^{19}F signals. By exploring this, a large number of ^{19}F containing biosensors have been reported for the detection of enzymes,[12,13] reactive oxygen species,[14,15] metal ions,[16] and small organic analytes.[17,18] Another strategy through which ^{19}F-based biosensors were designed is by modulating the transverse relaxation time (T_2) of ^{19}F through the paramagnetic relaxation enhancement (PRE) effect. Several ^{19}F ON/OFF probes have been reported for the detection of enzyme activity[19–22] and nucleotides[23] by modulating the T_2 relaxation by using the PRE effect. Yet another strategy by which the T_2 relaxation can be modulated is through the restriction of molecular motions by self-assembling the probe. This was applied for the design of several assembly–disassembly-driven ^{19}F ON/OFF probes for the detection and imaging of proteins.[24–28] Though highly promising, no attempt has been made yet to develop a ^{19}F-based biosensor for the detection of cancer biomarkers.

Herein, we report a universal supramolecular approach for the crafting of a ^{19}F ON/OFF *in vitro* biosensor for the detection of ssDNA binding cancer biomarkers. Our strategy involves the initial electrostatic assembly between negatively charged cancer biomarker binding ssDNA (hydrophilic segment) and a cationic ^{19}F probe (hydrophobic segment), leading to the formation of a supramolecular DNA amphiphile with the cationic ^{19}F probe tethered along the anionic backbone of ssDNA.[29–35] Subsequent self-assembly of the supramolecular amphiphile results in the formation of soft nanoparticles (NPs). The key to our design strategy is that in the self-assembled state with almost complete arrest of the molecular motions of the ^{19}F probe moiety, the characteristic ^{19}F signal of the probe has completely vanished (OFF state) due to the significant shortening of T_2 relaxation. On the other hand, molecular recognition of ssDNA by the cancer biomarkers results in the disassembly of the NPs and the simultaneous

School of Chemistry, Indian Institute of Science Education and Research (IISER) Thiruvananthapuram, Trivandrum 695541, Kerala, India.
E-mail: reji@iisertvm.ac.in

† Electronic supplementary information (ESI) available. See DOI: https://doi.org/10.1039/d3nr01175e

release of the free probe. This disassembly causes the restoring of the characteristic ^{19}F signal of the probe (ON state). The universal nature of our approach is demonstrated through the detection of various cancer biomarkers including miRNA (miRNA-21), ATP (small molecule-based biomarker), thrombin (enzyme-based biomarker), and telomerase (enzyme-based biomarker) (Scheme 1).

Synthesis of the cationic hydrophobic probe **1** is provided in the ESI.† Target cancer biomarkers selected in our study include thrombin,[36] adenosine triphosphate (ATP),[37] telomerase enzyme,[38] and miRNA-21 [39] (Table 1). Accordingly, we have selected **DNA1** (ATP binding aptamer), **DNA2** (thrombin binding aptamer), **DNA4** (complementary DNA to miRNA-21), and **DNA5** (telomerase primer) as the target DNAs for the biomarkers. **DNA3** is having two base mismatches with respect to the thrombin binding aptamer (**DNA2**), hence it acts as a control DNA to study the specificity of the aptamer binding to thrombin. Details of the synthesis and characterization of all DNAs are provided in the ESI.† Thrombin, ATP, and miRNA-21 were commercially purchased and used as such. Telomerase enzyme was extracted from HeLa cell lines by following a reported procedure.[40]

Noncovalent synthesis of supramolecular amphiphiles was achieved by annealing **1** (60 or 30 μM) and DNA (6 or 3 μM) at a molar ratio of 10 : 1 in D_2O at 90 °C for 10 minutes followed by slow cooling to room temperature at a cooling rate of 5 °C per minute over a period of 10 h. This particular procedure was adopted considering the uniform formation of NPs. Dynamic light scattering (DLS) analyses of **DNA1**/**1** showed the formation of aggregated species in solution with a size distribution in the range of 60–615 nm (Fig. 1a). As expected, zeta

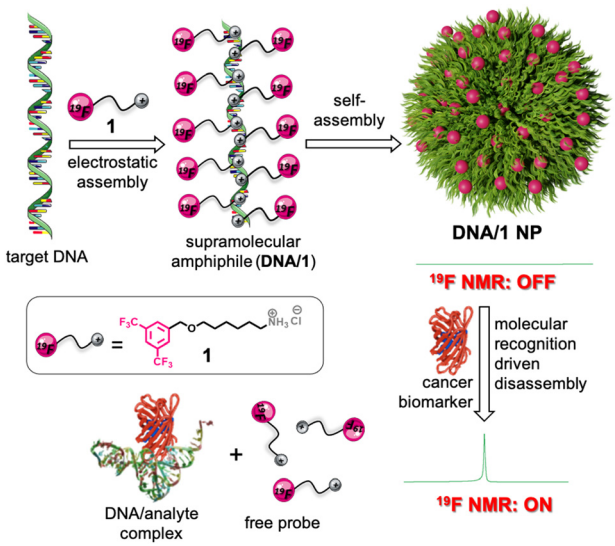

Scheme 1 Schematic representation illustrating the synthesis of a supramolecular amphiphile by the electrostatic assembly between the negatively charged DNA and the positively charged ^{19}F probe **1**. The subsequent self-assembly of the amphiphile into ^{19}F NMR silent (OFF state) NPs is shown. Schematic depiction of the molecular recognition-driven disassembly of the NPs and the subsequent ^{19}F NMR 'turn ON' response.

Table 1 Sequence of DNAs

DNA	Sequence (3′ → 5′)	Target
DNA1	ACCTGGGGGAGTATTGCGGAGGAAGGT	ATP
DNA2	GGTTGGTGTGGTTGG	Thrombin
DNA3	GGTTGCTGTAGTTGG	Scrambled
DNA4	TCAACATCAGTCTGATAAGCTA	miRNA-21
DNA5	AATCCGTCGAGCAGAGTT	Telomerase

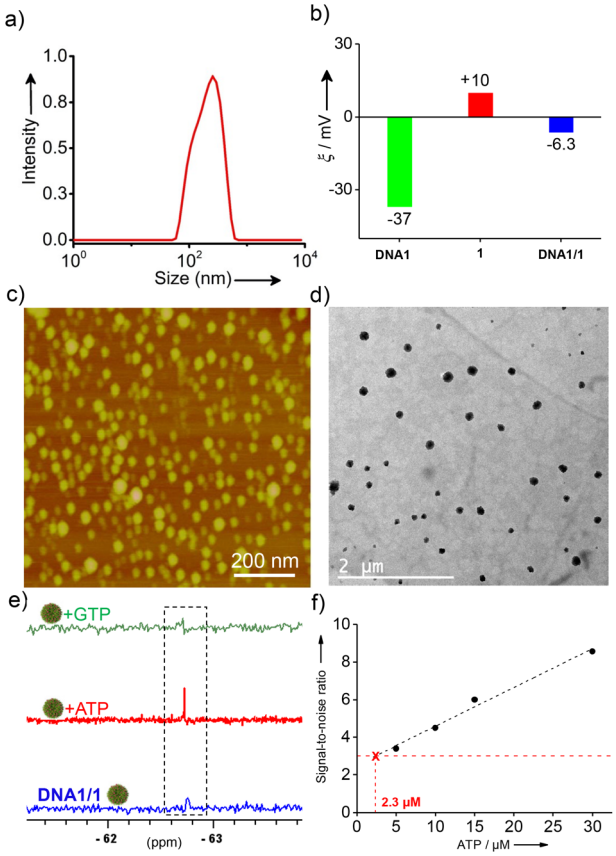

Fig. 1 (a) DLS, (b) zeta potential, (c) AFM and (d) TEM analyses of **DNA1**/**1** (1 : 10 molar ratio) NPs. (e) ^{19}F-NMR spectral responses of **DNA1**/**1** NPs (6 μM) with the addition of ATP (60 μM) and GTP (1 mM). (f) A plot of the ^{19}F NMR signal-to-noise ratio *versus* the concentration of ATP (0 → 30 μM) using **DNA1**/**1** NPs (3 μM). The corresponding LoD value for ATP detection is also shown in the figure.

potential measurements of **DNA1** and **1** revealed values of −37.0 mV and +10.0 mV, respectively. Interestingly, a zeta potential value of −6.3 mV was observed for the aggregates of **DNA1**/**1** (Fig. 1b). This almost neutral zeta potential value for **DNA1**/**1** aggregates clearly indicates that the assembly between negatively charged DNA and positively charged **1** leads to the formation of almost neutral aggregated species in solution. Atomic force microscopy (AFM) (Fig. 1c) and transmission electron microscopy (TEM) (Fig. 1d) analyses of **DNA1**/**1** showed the formation of spherical NPs. These observations conclude that the supramolecular assembly between **DNA1** and **1** results in the formation of supramolecular amphiphiles (**DNA1**/**1**) by

the non-covalent tethering of **1** along the anionic backbone of DNA through the strong electrostatic attraction. Subsequent self-assembly of the supramolecular amphiphile (**DNA1**/**1**) *via* hydrophobic and π-stacking interactions results in the formation of spherical NPs with the ^{19}F containing hydrophobic moiety buried inside the NPs with no/minimum contact with the polar medium.

The first cancer biomarker we targeted in our study was ATP. ^{19}F NMR studies of the cationic probe **1** at a concentration of 60 μM in D_2O revealed a sharp singlet at −67.72 ppm due to the presence of two magnetically equivalent $-CF_3$ groups. Interestingly, a reduction in the intensity of the peak at −67.72 ppm was observed with the addition of **DNA1** and the peak completely vanished at a concentration of 6 μM of **DNA1** (Fig. S5a†). This suggests that the NPs synthesized at a molar ratio 1 : 10 of **DNA1** and **1** is ^{19}F NMR silent due to the significant reduction of T_2 relaxation caused by the complete arrest of the molecular motions of the probe in the aggregated state. Accordingly, the 1 : 10 molar ratio of **DNA1** and **1** was used for further experiments. Stability of the NPs is an extremely important requirement in our design strategy as the undesired disassembly of the NPs and the resulting emergence of the ^{19}F signal may leads to wrong prediction. Stability of the NPs was then investigated under different conditions. Interestingly, no change was observed in the ^{19}F NMR spectra of **DNA1**/**1** NPs with time (0 → 48 h), temperature (25 °C → 85 °C) and pH (5.5 → 8.5), revealing that the NPs are stable with respect to time, temperature and pH (Fig. S5b–d†). Furthermore, no significant change was observed for the DLS size distribution of the NPs with respect to pH, time and temperature (Fig. S6a–c†). These results confirm that the NPs are stable and the possibility of their undesired disassembly is very unlikely.

After establishing the stability of the NPs, we then enduced the interaction of **DNA1**/**1** NPs with ATP by gradually adding ATP into the NP solution and the emergence of the ^{19}F NMR signal was monitored. Interestingly, emergence of the characteristic ^{19}F NMR peak of **1** at −67.72 ppm was observed with the addition of ATP into the **DNA1**/**1** NP solution and an intense sharp singlet was observed with the addition 60 μM of ATP (Fig. 1e). These results clearly reveal that specific molecular recognition between ATP and **DNA1** results in the disassembly of **DNA1**/**1** NPs with the simultaneous formation of an ATP/**DNA1** complex. This in turn disassembles the supramolecular amphiphile (**DNA1**/**1**) and releases the monomeric probe **1**. This molecular recognition-driven disassembly leads to the 'turn ON' of the ^{19}F NMR signal of the probe. Circular dichroism (CD) analyses revealed that **DNA1** adopted a random coil conformation in the NP state as no specific CD signal was observed.[41] However, after binding to ATP, an intense positive CD signal at 290 nm was clearly observed, indicating the formation of an antiparallel G-quadruplex conformation (Fig. S7†).[41] This conformational switching of **DNA1** from a random coil to an antiparallel G-quadruplex supports the binding of **DNA1** with ATP. As expected, no 'turn ON' of the ^{19}F NMR response was observed with the addition of guanosine-5′-triphosphate (GTP) (Fig. 1e), which clearly support our hypothesis that the specific molecular recognition between **DNA1** and ATP is solely responsible for the disassembly of the NPs and the subsequent ^{19}F NMR 'turn ON' response. Subsequently, we have determined the limit of detection (LoD) of the probe by titrating the **DNA1**/**1** NPs with varying concentrations of ATP.[42] For this, the ^{19}F NMR silent **DNA1**/**1** NPs (3 μM) were treated with increasing concentration of ATP (0 → 30 μM) and the signal-to-noise ratio of the ^{19}F peak emerged at −67.72 ppm was plotted against the concentration of ATP. The LoD value for the detection of ATP was found to be 2.3 μM, which is well below the concentration range of ATP typically present inside the cancer cells.[43]

To establish the universal nature of the system for the detection of various cancer biomarkers, we have explored the detection of other potential cancer biomarkers including thrombin and miRNA-21. **DNA2** was selected as the target for thrombin detection, which is a 15-mer thrombin binding DNA aptamer. Towards this, **DNA2**/**1** NPs (6 : 60 μM) were first synthesized by following the general procedure. Nanoparticle formation was characterized using DLS (Fig. S3†), AFM (Fig. 2a) and TEM (Fig. 2b) analyses. DLS size distribution analyses revealed that the size of the NPs is in the range of 140–460 nm. As expected, the **DNA2**/**1** NPs were ^{19}F NMR silent (Fig. 2c). Interestingly, the addition of thrombin into the **DNA2**/**1** NP solution showed the emergence of the characteristic ^{19}F NMR peak of **1** at −67.72 ppm (Fig. 2c) and a sharp

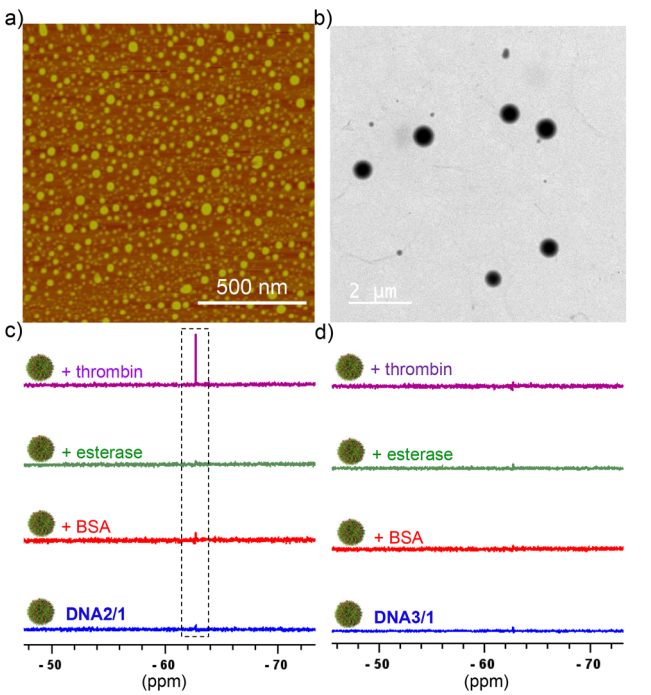

Fig. 2 (a) AFM and (b) TEM images of (a) **DNA2**/**1** NPs (6 : 60 μM). (c) ^{19}F NMR response of **DNA2**/**1** (6 : 60 μM) NPs with the addition of different proteins including BSA (5 μM), esterase (5 μM) and thrombin (5 μM). (d) ^{19}F NMR response of **DNA3**/**1** (6 : 60 μM) NPs with the addition of different proteins including BSA (5 μM), esterase (5 μM) and thrombin (5 μM).

singlet at −67.72 ppm was observed with the addition of 5 μM of thrombin. This indicates that the molecular recognition between **DNA2** and thrombin leads to the formation of a **DNA2**/thrombin complex, which in turn results in the disassembly of the NPs and releases the monomeric probe **1**. As expected, no 'turn ON' of the ^{19}F NMR response was observed with the addition of other enzymes such as BSA and esterase (Fig. 2c), which clearly support our hypothesis that the specific molecular recognition between **DNA2** and thrombin is solely responsible for the disassembly of the NPs and the subsequent ^{19}F NMR 'turn ON' response. Furthermore, no 'turn ON' response was observed for the **DNA3**/**1** NPs with the addition of thrombin, BSA or esterase, disclosing that **DNA2** (scrambled DNA sequence) has no interaction with any of the proteins and hence no molecular recognition-driven disassembly of the NPs (Fig. 2d).

For the detection of miRNA-21, **DNA4** was designed, which is fully complementary to miRNA-21. Subsequently, **DNA4**/**1** (6 : 60 μM) NPs were synthesized and characterized by using various microscopic (Fig. 3b) and light scattering techniques (Fig. S3†). The average diameter of the particles from DLS analyses was found to be 125 nm. As expected, the NPs were ^{19}F NMR silent due to the significant shortening of T_2 relaxation (Fig. 3c). Interestingly, the characteristic singlet at −67.72 ppm of the probe emerged with the addition of miRNA-21 (Fig. 3c). This can be attributed to the duplex formation between **DNA4** and miRNA-21, which in turn releases the probe **1** into the solution and thereby 'turning ON' the ^{19}F NMR signal.

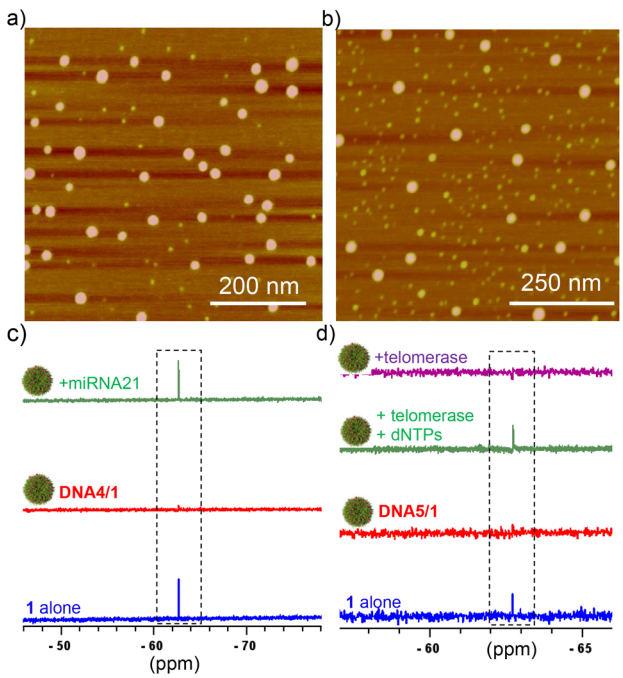

Fig. 3 AFM images of (a) **DNA4**/**1** and (b) **DNA5**/**1** NPs (6 : 60 μM). ^{19}F-NMR spectral responses of (c) **DNA4**/**1** NPs with the addition of miRNA-21 (90 μM) and (d) ^{19}F-NMR spectral changes of **DNA5**/**1** NPs with the addition of telomerase and dNTPs and telomerase alone (4 h of incubation).

In order to demonstrate that our approach can be applied for practical applications, we have extended our study to the detection of telomerase activity (another potential cancer biomarker), that is directly extracted from cultured HeLa cells. For this purpose, **DNA5** was designed, which is a short 22-mer telomerase primer and hence the primer ssDNA can be extended at its 3′-end by the telomerase enzyme to produce telomeric repeat sequences. Keeping this in mind, we initially synthesized **DNA5**/**1** (6 : 60 μM) NPs and characterized using microscopic (Fig. 3b) and light scattering analyses (Fig. S3†). The average diameter of the particle is 60 nm from the DLS analysis. As anticipated, the **DNA5**/**1** NPs were ^{19}F NMR silent due to the shortening of T_2 relaxation (Fig. 3d). The NPs were then incubated with deoxynucleotide triphosphates (dNTPs: dATP, dGTP, dCTP and dTTP; 100 μM each) and telomerase (10 μL from the extract of ~2.5 × 10^6 cells) in phosphate-buffered saline (pH 7.5) for different time intervals. No appearance of the characteristic ^{19}F NMR peak was observed in 10 minutes of incubation, indicating that the **DNA5**/**1** NPs are still in the self-assembled state. However, the characteristic peak of **1** at −67.72 ppm emerged after 4 h of incubation, implying that the NPs are completely dissociated and caused the 'turn ON' of the ^{19}F NMR signal (Fig. 3d). In the presence of telomerase and dNTPs, the telomerase primer (**DNA5**) is getting elongated from its 3′-end to produce the corresponding telomeric repeat sequences, which in turn transforms the supramolecular amphiphile (**DNA5**/**1**) into a longer hydrophilic ssDNA. This causes the disassembly of the NPs and leads to the 'turn ON' of the ^{19}F NMR signal. No emergence of the ^{19}F NMR signal was observed when the NPs were incubated just with the telomerase enzyme, indicating that primer elongation requires both telomerase and dNTPs (Fig. 3d).

In order to check the performance of the probe in a complex mixture of potential nontargets, we have carried out the detection of the analytes in the presence of other potential nontargets. For this purpose, **DNA1**/**1** (probe for ATP), **DNA2**/**1** (probe for thrombin) and **DNA5**/**1** (probe for telomerase) NPs were prepared as described and their response was studied in the presence of a mixture of other targets. Initially, the response of **DNA1**/**1** NPs towards ATP was studied. As expected, the **DNA1**/**1** (6 : 60 μM) NPs were ^{19}F NMR silent and no ^{19}F NMR 'turn ON' response was observed with the addition of a mixture of other potential targets including thrombin (5 μM), telomerase (10 μL from the extract of ~2.5 × 10^6 cells) and miRNA (10 μM). However, a strong 'turn ON' response was observed with the addition of ATP (100 μM, target cancer biomarker in this case) (Fig. 4a). This clearly reveals that our probe is highly specific to the target and is responsive even in the presence of a mixture of nontargets. Similarly, **DNA2**/**1** (6 : 60 μM) was ^{19}F NMR silent in the presence of a mixture of ATP (100 μM), telomerase (10 μL from the extract of ~2.5 × 10^6 cells) and miRNA (10 μM), but a strong ^{19}F NMR signal emerged with the addition of target thrombin (5 μM) (Fig. 4b). The same observations were made for telomerase detection as well. The ^{19}F NMR silent **DNA5**/**1** (6 : 60 μM) NPs in a mixture of ATP (100 μM), thrombin (5 μM), and miRNA (10 μM) showed

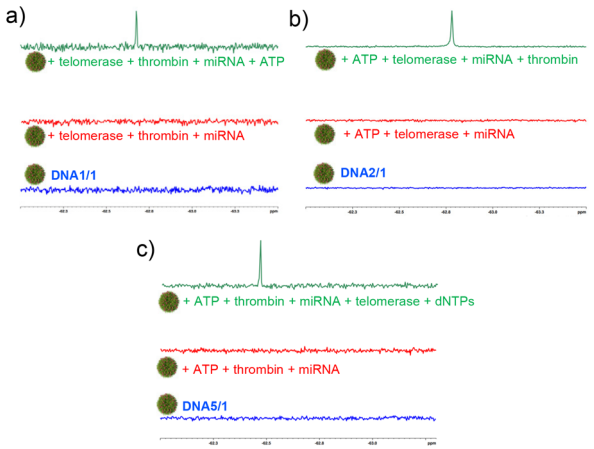

Fig. 4 ^{19}F-NMR spectral responses of (a) **DNA1/1** NPs towards ATP, (b) **DNA2/1** NPs towards thrombin and (c) **DNA5/1** NPs towards telomerase in the presence of a mixture of other nontargets.

the emergence of a strong ^{19}F NMR signal with the addition of target telomerase (10 μL from the extract of ~2.5 × 10^6 cells) along with dNTPs: dATP, dGTP, dCTP and dTTP (100 μM each) (Fig. 4c).

In summary, we have demonstrated a supramolecular approach for the design of assembly–disassembly-driven ^{19}F ON/OFF NPs triggered by specific molecular recognition for the detection of ssDNA binding cancer biomarkers with excellent selectivity. To the best of our knowledge, this is the first report demonstrating the potential of ^{19}F ON/OFF NPs for the specific detection of DNA binding cancer biomarkers *in vitro*. The universal nature of our approach is demonstrated through the detection of different types of targets including thrombin, ATP, miRNA, and telomerase. Because the molecular recognition between DNA and the analyte is highly specific in nature, this strategy offers excellent selectivity. Unlike the known ^{19}F NMR probes, where the detection of different analytes involves the laborious synthetic modification of the probe, our approach is modular in nature and permits the detection of any DNA-based analyte with a single ^{19}F NMR probe. Though unique in many ways, it is to be mentioned that the sensitivity of ^{19}F NMR-based systems is considerably lower when compared to the traditional ^{1}H-MRI probes. However, this can be addressed to a large extent by the appropriate molecular design of the ^{19}F probe and improvement in the NMR instrumentation, and the ^{19}F-MRI technique can emerge as a dominant tool for *in vivo* imaging applications. We hope that the universal nature and less laborious non-covalent strategy demonstrated here may encourage other researchers to explore this for the detection of other DNA-binding analytes for disease diagnosis and *in vivo* imaging applications.

Conflicts of interest

There are no conflicts to declare.

Acknowledgements

Financial supports from DBT (BT/PR30172/NNT/28/1593/-2018) and CSIR (Research Fellowship) are acknowledged.

References

1 K. A. Cronin, A. J. Lake, S. Scott, R. L. Sherman, A. M. Noone, N. Howlader, S. J. Henley, R. N. Anderson, A. U. Firth, J. Ma, B. A. Kohler and A. Jemal, *Cancer*, 2018, **124**, 2785–2800.
2 L. Wuab and X. Qu, *Chem. Soc. Rev.*, 2015, **44**, 2963–2997.
3 M. Perfezou, A. Turner and A. Merkoci, *Chem. Soc. Rev.*, 2012, **41**, 2606–2622.
4 A. B. Chinen, C. M. Guan, J. R. Ferrer, S. N. Barnaby, T. J. Merkel and C. A. Mirkin, *Chem. Rev.*, 2015, **115**, 10530–10574.
5 B. V. Chikkaveeraiah, A. A. Bhirde, N. Y. Morgan, H. S. Eden and X. Chen, *ACS Nano*, 2012, **6**, 6546–6561.
6 R. de la Rica and M. M. Stevens, *Nat. Nanotechnol.*, 2012, **7**, 821–824.
7 S. A. Kazane, D. Sok, E. H. Cho, M. L. Uson, P. Kuhn, P. G. Schultz and V. V. Smider, *Proc. Natl. Acad. Sci. U. S. A.*, 2012, **109**, 3731–3736.
8 S. R. Panikkanvalappil, M. A. Mackey and M. A. El-Sayed, *J. Am. Chem. Soc.*, 2013, **135**, 4815–4821.
9 S. Mizukami, R. Takikawa, F. Sugihara, Y. Hori, H. Tochio, M. W. Lchli, M. Shirakawa and K. Kikuchi, *J. Am. Chem. Soc.*, 2008, **130**, 794–795.
10 M. Srinivas, P. A. Morel, L. A. Ernst, D. H. Laidlaw and E. T. Ahrens, *Magn. Reson. Med.*, 2007, **58**, 725–734.
11 E. T. Ahrens, B. M. Helfer, C. F. O'Hanlon and C. Schirda, *Magn. Reson. Med.*, 2014, **72**, 1696–1701.
12 W. Cui, P. Otten, Y. Li, K. S. Koeneman, J. Yu and R. P. Mason, *Magn. Reson. Med.*, 2004, **51**, 616–620.
13 M. R. Baranowski, A. Nowicka, A. M. Rydzik, M. Warminski, R. Kasprzyk, B. A. Wojtczak, J. Wojcik, T. D. W. Claridge, J. Kowalska and J. Jemielity, *J. Org. Chem.*, 2015, **80**, 3982–3997.
14 A. R. Lippert, G. C. Van De Bittner and C. J. Chang, *Acc. Chem. Res.*, 2011, **44**, 793–804.
15 K. J. Bruemmer, S. Merrikhihaghi, C. T. Lollar, S. N. S. Morris, J. H. Bauer and A. R. F. Lippert, *Chem. Commun.*, 2014, **50**, 12311–12314.
16 G. A. Smith, R. T. Hesketh, J. C. Metcalfe, J. Feeney and P. G. Morris, *Proc. Natl. Acad. Sci. U. S. A.*, 1983, **80**, 7178–7182.
17 Y. Zhao, G. Markopoulos and T. M. Swager, *J. Am. Chem. Soc.*, 2014, **136**, 10683–10690.
18 Y. Zhao, L. Chen and T. M. Swager, *Angew. Chem., Int. Ed.*, 2016, **55**, 917–921.
19 S. Mizukami, R. Takikawa, F. Sugihara, Y. Hori, H. Tochio, M. Wälchli, M. Shirakawa and K. Kikuchi, *J. Am. Chem. Soc.*, 2008, **130**, 794–795.

20 S. Mizukami, H. Matsushita, R. Takikawa, F. Sugihara, M. Shirakawa and K. F. Kikuchi, *Chem. Sci.*, 2011, **2**, 1151–1155.
21 H. Matsushita, S. Mizukami, Y. Mori, F. Sugihara, M. Shirakawa, Y. Yoshioka and K. F. Kikuchi, *ChemBioChem*, 2012, **13**, 1579–1583.
22 S. Mizukami, R. Takikawa, F. Sugihara, M. Shirakawa and K. Kikuchi, *Angew. Chem., Int. Ed.*, 2009, **48**, 3641–3643.
23 M. E. Dempsey, H. D. Marble, T.-L. Shen, N. L. Fawzi and E. M. Darling, *Bioconjugate Chem.*, 2018, **29**, 335–342.
24 Y. Takaoka, T. Sakamoto, S. Tsukiji, M. Narazaki, T. Matsuda, H. Tochio, M. Shirakawa and I. Hamachi, *Nat. Chem.*, 2009, **1**, 557–561.
25 Y. Takaoka, K. Kiminami, K. Mizusawa, K. Matsuo, M. Narazaki, T. Matsuda and I. Hamachi, *J. Am. Chem. Soc.*, 2011, **133**, 11725–11731.
26 K. Matsuo, R. Kamada, K. Mizusawa, H. Imai, Y. Takayama, M. Narazaki, T. Matsuda, Y. Takaoka and I. Hamachi, *Chem. – Eur. J.*, 2013, **19**, 12875–12883.
27 Y. Yuan, S. Ge, H. Sun, X. Dong, H. Zhao, L. An, J. Zhang, J. Wang, B. Hu and G. Liang, *ACS Nano*, 2015, **9**, 5117–5124.
28 J. M. Perez, L. Josephson, T. O'Loughlin, D. Högemann and R. Weissleder, *Nat. Biotechnol.*, 2002, **20**, 816–820.
29 M. A. Azagarsamy, P. Sokkalingam and S. Thayumanavan, *J. Am. Chem. Soc.*, 2009, **131**, 14184–14185.
30 B. Narayan, S. P. Senanayak, A. Jain, K. S. Narayan and S. J. George, *Adv. Funct. Mater.*, 2013, **23**, 3053–3060.
31 C. Rest, M. J. Mayoral, K. Fucke, J. Schellheimer, V. Stepanenko and G. Fernández, *Angew. Chem., Int. Ed.*, 2014, **53**, 700–705.
32 S. Ghosh, D. S. Philips, A. Saeki and A. Ajayaghosh, *Adv. Mater.*, 2017, **29**, 1605408.
33 A. Mukherjee, T. Sakurai, S. Seki and S. Ghosh, *Langmuir*, 2020, **36**, 13096–13103.
34 S. K. Albert, M. Golla, N. Krishnan, D. Perumal and R. Varghese, *Acc. Chem. Res.*, 2020, **53**, 2668–2679.
35 S. K. Albert, I. Sivakumar, M. Golla, H. V. P. Thelu, N. Krishnan, K. L. J. Libin, Ashish and R. Varghese, *J. Am. Chem. Soc.*, 2017, **139**, 17799–17802.
36 M. Lundbech, A. E. Krag, T. D. Christensen and A.-M. Hvas, *Thromb. Res.*, 2020, **186**, 80–85.
37 S. Zhang, Y. Yan and S. Bi, *Anal. Chem.*, 2009, **81**, 8695–8701.
38 X. Lou, Y. Zhuang, X. Zuo, Y. Jia, Y. Hong, X. Min, Z. Zhang, X. Xu, N. Liu, F. Xia and B. Z. Tang, *Anal. Chem.*, 2015, **87**, 6822–6827.
39 Y. Wang, D. Zheng, Q. Tan, M. X. Wang and L.-Q. Gu, *Nat. Nanotechnol.*, 2011, **6**, 668–674.
40 R. Qian, L. Ding, L. Yan, M. Lin and H. Ju, *J. Am. Chem. Soc.*, 2014, **136**, 8205–8208.
41 S. Yan, R. Huang, Y. Zhou, M. Zhang, M. Deng, X. Wang, X. Weng and X. Zhou, *Chem. Commun.*, 2011, **47**, 1273–1275.
42 M. E. Dempsey, H. D. Marble, T.-L. Shen, N. L. Fawzi and E. M. Darling, *Bioconjugate Chem.*, 2018, **29**, 335–342.
43 X.-R. Song, S.-H. Li, H. Guo, W. You, D. Tu, J. Li, C.-H. Lu, H.-H. Yang and X. Chen, *Adv. Sci.*, 2018, **5**, 1801201.